Jordan Journal of Civil Engineering, Volume **18**, No. **3**, **2024**
DOI: https://doi.org/10.14525/JJCE.v18i3.09

Jordan Journal of Civil Engineering

Journal homepage: https://jjce.just.edu.jo

Reliability Analysis of Hillslopes under Different Rainfall Patterns

Adarsh S. Chatra [1)]****, Ramanandan, S.*** [2)]***, Sundaravel, V.*** [2)] ***and V. B. Maji*** [3)]

[1)] *Associate Professor, Department of Civil Engineering, Basaveshwar Engineering College, Bagalkot, Karnataka, India.*
** Corresponding Author. E-Mail: adarshchatra@gmail.com*
[2)] *Research Scholar, Department of Civil Engineering, Indian Institute of Technology Madras, Chennai, India.*
[3)] *Associate Professor, Department of Civil Engineering, Indian Institute of Technology Madras, Chennai, India.*

ARTICLE INFO

Article History:
Received: 14/12/2023
Accepted: 24/5/2024

ABSTRACT

Rainfall-induced slope failures and landslides pose significant hazards worldwide, impacting various regions, including the Kurumbadi area of Nilgiris, Tamil Nadu, India. Despite the region's vulnerability to such disasters, limited research has addressed the uncertainties surrounding soil parameters, particularly in the context of slope-stability analysis. The present study aims to fill this gap by conducting reliability analysis to assess the stability of hillslopes under different rainfall patterns. It specifically investigates how variations in soil compaction, including medium dense and loose soils, influence slope stability under both advanced and recorded rainfall patterns in the Kurumbadi area. Utilizing data from numerical analyses using Fast Lagrangian Analysis of Continua (FLAC), the study conducts comprehensive reliability analysis with Response Surface Methodology (RSM) and First-order Reliability Method (FORM), to evaluate slope stability. The findings reveal that advanced rainfall patterns significantly increase the likelihood of slope failure, highlighting the region's increased vulnerability to intense rainfall events. These insights contribute valuable knowledge to the assessment of slope instability across varying rainfall intensities and durations. Furthermore, the findings support the development of proactive measures, such as early-warning systems based on predefined threshold values, to mitigate the risks associated with rainfall-induced slope failures.

Keywords: Rainfall patterns, Slope failures, Nilgiris, Probability of failure, Reliability.

INTRODUCTION

Frequent rainfall-induced landslides present substantial global risks as natural disasters. Rainwater infiltrates the slopes resulting in an increase of pore-water pressure causing a reduction in the shear strength of the soil. Increased human settlement on the hillslopes in Nilgiris district of Tamil Nadu, India, alongside rising construction and vehicle activity, pose serious threats of rain-induced slope failures. Landslides are frequent along these hillslopes and occur almost every year, posing threats to lives and properties. The Factor of Safety (FOS) is defined in slope-stability analysis as the ratio of resisting moment to driving moment. The parameters used to evaluate the FOS of slopes subjected to rainwater infiltration are uncertain, which eventually makes the FOS unreliable. Several researchers have performed deterministic and non-deterministic studies to address real-time problems faced in the geotechnical-engineering field (Bouatia et al., 2023; Raouf and Bahloul, 2023). The conventional deterministic stability analysis neglects these uncertainties (Cai and Ugai, 2004; Chatra et al., 2017; Wu and Hsieh, 2021; Shou et al., 2018, Eichenberger et al., 2013). Probabilistic approaches provide a rational way to account for the uncertainties from different sources (Wu et al., 2021; Liao and Ji, 2021, Kim et al., 2021, Wu et al., 2020; Christian et al., 1994; Duncan, 2000; Wu and Kraft, 1970; Santoso et al., 2011).

In the context of rainfall-induced slope-stability analysis, the mechanical and hydraulic parameters of the soil are considered as random variables with their respective probability distributions, rather than considering a constant deterministic value (Kim et al., 2021; Huang et al., 2023; Babu and Murty, 2005; Cai et al., 2017). Several studies in the past have performed the reliability analysis of natural slopes under rainfall conditions (Ali et al. 2014; Cho, 2019; Martinovic et al., 2017; Liao and Ji, 2021, Kim et al., 2021). The current study focuses on conducting reliability analysis of a hillslope segment situated in Kurumbadi village, within the Nilgiris region (referred to as the Kurumbadi slope). The effect of rainfall on the FOS of hillslopes is evaluated using the finite-difference code, Fast Lagrangian Analysis of Continua (FLAC). The Response Surface Methodology (RSM) in combination with FLAC analysis and First-order Reliability Method (FORM) are utilized to perform reliability analyses. The primary emphasis of the current study is twofold: (a) investigating the impact of rainfall on hillslope stability while accounting for soils with varying degrees of compaction and (b) quantifying hillslope stability through the calculation of the probability of failure (P_f) for both recorded and advanced rainfall patterns.

METHODOLOGY

Description of the Study Area

The study area selected for the present study is shown schematically in Fig. 1. The site is located at slope section (N 11° 20' 15.2" and E 76° 50' 0.6") from the Kurumbadi village area, the Nilgiris district of Tamil Nadu, India. The sub-tropical climate and intense physical and chemical weathering have resulted in a thick yellowish to reddish brown soil found near the ground surface (Jaiswal et al., 2010). The area consists of charnockite rocks and gneisses of Archaean age (Seshagiri and Badarinarayanan, 1982). These rocks are overlain by the ubiquitous red laterite or lateritic soils. The charnockite is garnetiferous and its outcrops are well-exposed along the cut slopes of road, railroad and landslide scarps. Field observations have indicated that a relatively thin surface soil with an average thickness of 3 m overlies an impermeable layer; i.e., charnockite rock. The failure planes are slightly irregular, but are approximately parallel to the ground slope surface.

Numerical-simulation Procedure

In this study, the simulation of rainwater infiltration utilizes a two-phase flow approach implemented through FLAC (2011). The two phases involved are water and air, occupying the void space. The flow dynamics of both fluids are described by Darcy's law, which governs the movement of water and air within the system, which is given by:

$$q_w = -k_w\, k_{rw}\, \frac{\partial}{\partial x}\, (P_w - \rho_w\, g\, x) \qquad (1)$$

$$q_g = -k_w\, \frac{\mu_w}{\mu_g}\, k_{rg}\, \frac{\partial}{\partial x}\, \left(P_g - \rho_g\, g\, x\right) \qquad (2)$$

where q_w and q_g are the fluid flow of water and air, respectively, k_w is the mobility coefficient which is a function of saturated permeability (k_s), κ_{rw} and κ_{rg} are the relative mobilities of water and air, respectively. P_w and P_g are the pore-water and pore-air pressures, respectively, ρ_w and ρ_g are the water and air densities, respectively, μ_w and μ_g are the dynamic viscosities of water and air, respectively and g is the acceleration due to gravity, while x indicates the direction of flow.

Formulating an accurate model for rain-induced seepage and slope-stability analysis in partially saturated soil is essential. The model needs to appropriately capture the complexities of moisture infiltration and its impact on slope stability. Careful consideration should be given to factors, such as soil-saturation levels, pore-water pressure changes and variations in soil properties. A comprehensive formulation should integrate relevant hydrological principles and geotechnical factors to ensure a realistic representation of the dynamic interactions between rainfall, seepage and slope stability in partially-saturated soil. The governing differential equations for subsurface flow are expressed as:

$$n\left[\frac{S_w}{K_w}\frac{\partial P_w}{\partial t}+\frac{\partial S_w}{\partial t}\right]=-\left[\frac{\partial q_w}{\partial x}+S_w\frac{\partial \varepsilon}{\partial t}\right] \quad (3)$$

$$n\left[\frac{S_g}{K_g}\frac{\partial P_g}{\partial t}+\frac{\partial S_g}{\partial t}\right]=-\left[\frac{\partial q_g}{\partial x}+S_g\frac{\partial \varepsilon}{\partial t}\right] \quad (4)$$

where q_w and q_g are the fluid flow of water and air, respectively. K_w and K_g are the bulk modulus of water and air, respectively. n is the porosity of the soil, ε is the volumetric strain and S_w and S_g are the saturation of water and air, respectively. The pore space is filled with two fluids related as:

$$S_w+S_g=1 \quad (5)$$

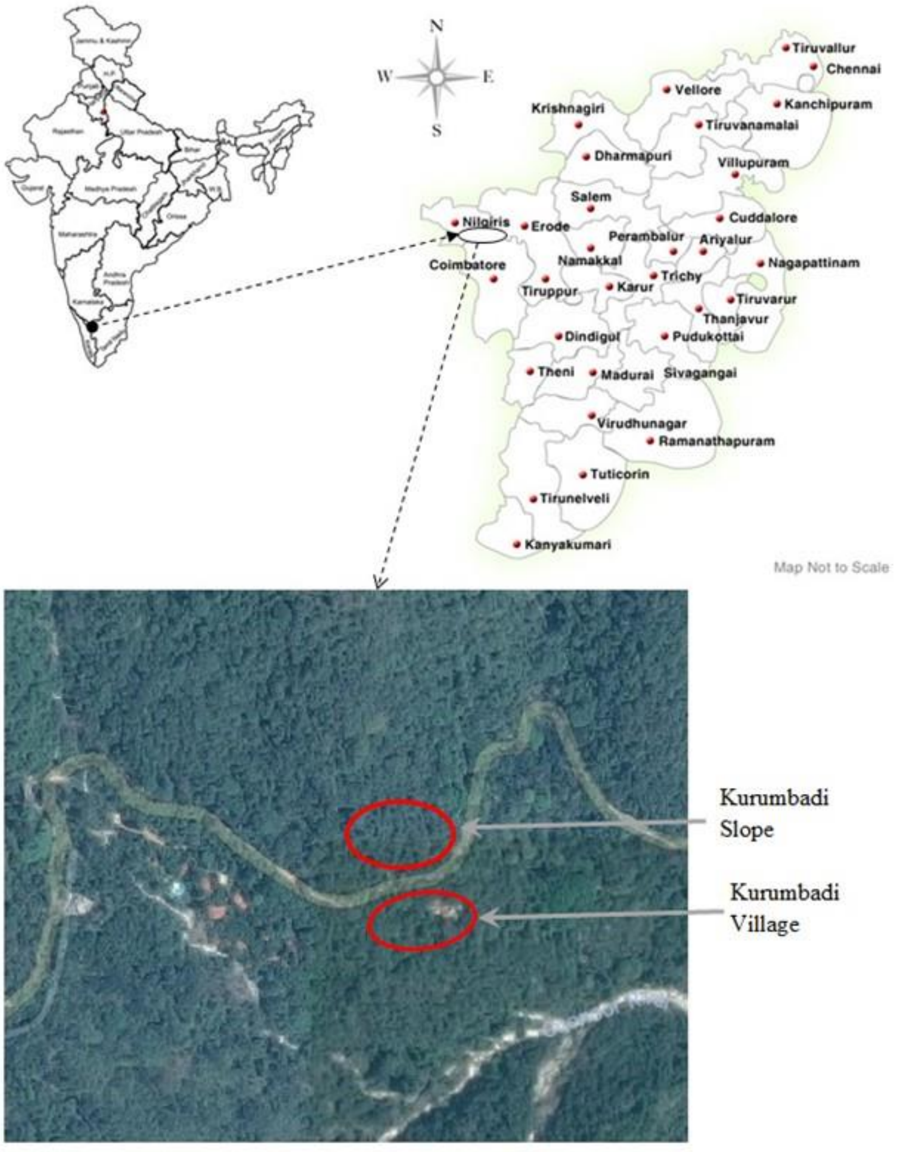

Figure (1): Location of Kurumbadi slope section, the Nilgiris district, Tamil Nadu, India

van Genuchten (1980) formulated a set of closed-form equations for representing the hydraulic characteristics of unsaturated soils, which are based on the capillary model of Mualem (1976). The equation for the Soil-Water Characteristic Curve (SWCC) is given as:

$$\Theta=\left(\frac{\theta-\theta_r}{\theta_s-\theta_r}\right)=\frac{1}{\left[1+\left(\frac{\omega}{P_0}\right)^m\right]^{1/1-m}} \quad (6)$$

where Θ is the relative degree of saturation, k_r is the relative permeability, θ is the volumetric water content, θ_s and θ_r are the saturated and residual volumetric water content, respectively, ω is the matric suction and P_0 and m are the van Genuchten curve fitting parameters. Capillary pressure is defined as the difference between air pressure and water pressure, which is a decreasing function of the saturation. An empirical expression of the van Genuchten form is used for the evaluation of capillary pressure (P_c) (FLAC Manual, 2011):

$$P_c = P_g - P_w = P_0\left[\Theta^{-1/m} - 1\right]^{1-m} \quad (7)$$

where P_0 is larger for finer materials and is a function of the surface tension, intrinsic permeability and porosity. In a fluid-only calculation, Equations (3), (4), (5) and (7) form a non-linear system of equations used to solve four unknowns; i.e., P_w, P_g, S_w and S_g, where air pressure is neglected in the present study. In two-phase flow calculation, P_w, P_g and one value of S_w are defined at each node. Using the weighting technique, contributions of nodal flow are calculated on zone basis. FLAC solves the non-linear system of equations with the help of additional equations for coupled fluid-mechanical calculations. These equations are boundary and initial conditions, balance of momentum, mechanical constitutive law and compatibility equation.

Slope-stability Analysis

Slope failures in the Nilgiris region are in general shallow translational slides, in which failure surface runs parallel to the ground surface. Therefore, infinite slope is chosen to analyze the stability of the unsaturated Kurumbadi slope in the Nilgiris region. The soil is 3 m deep underlain by bedrock. This limited depth of the soil covers on the hillslope favours translational slides. Figure 2 shows a typical infinite-slope model for which the FOS may be evaluated using shear-strength reduction (SSR) technique in FLAC commercial package. FLAC uses Finite Difference Method (FDM) to analyze and solve a wide range of geotechnical problems. The slope-stability computations are carried out in the present study using SSR technique. The rain-induced slope instability is assessed using FLAC with plain-strain analysis. The pore-water pressures needed in the calculation of shear strength of the unsaturated soils are obtained from the transient-flow analysis. Subsequently, the FOS calculations are performed utilizing the SSR technique by progressively reducing the shear strength of the soil (cohesion and friction) to bring the slope to a state of limiting equilibrium.

The soil slope is modelled using Mohr-Coulomb failure criterion. The SSR technique requires many trial runs with a trial factor of safety F_{trial} with c' and φ' adjusted as given by:

$$c' = \frac{1}{F_{trial}}\, c' \quad (8)$$

$$\varphi' = tan^{-1}\, \frac{1}{F_{trial}}\, tan\ \varphi'\ . \quad (9)$$

The F_{trial} value at which slope fails can be found using bracketing and bisection. Initially, upper and lower brackets are established. The simulation for the first converged F_{trial} is considered as lower bracket and non-convergence of F_{trial} is taken as upper bracket. Further, a point midway between convergence and non-convergence are tested. If the simulation converges, the new value is updated to the lower bracket and if the simulation does not converges, the upper bracket is replaced with the new value. The process is repeated until the difference between the upper and lower brackets is less than a particular tolerance value.

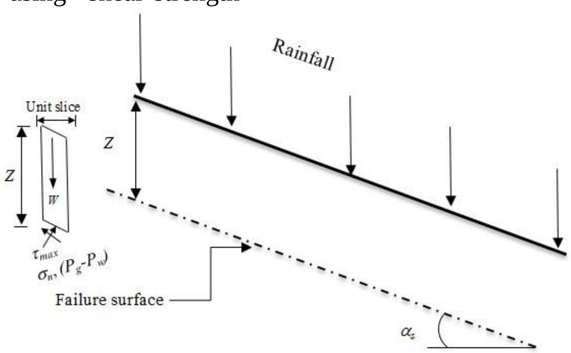

Figure (2): Infinite slope model

where Z = depth of soil mass, W = weight of slice, τ_{max} = maximum shear stress, σ_n = normal stress and α_s = slope angle.

Slope Properties

On November 10, 2009, Marapalam (near the case study site) in the Nilgiris district experienced a significant debris flow, resulting in loss of lives and extensive property damage. Geological survey of India reported recurring landslides during the second week of November annually. The 2009 event was notable and rainfall data from November 6th to 11th was analyzed. Standard Penetration Test (SPT) was performed at the slope location in Kurumbadi village and the soil samples were extracted at the selected locations within the site. The laboratory tests are performed to obtain the hydraulic properties and shear-strength parameters which are used in the stability analysis as shown in Table 1 and Table 2. The slope material, classified as silty sand (SM) over impermeable bedrock, experienced shallow rain-induced failures. Based on the SPT N-value, the soil is classified as a medium-dense soil.

To investigate the influence of relative density on slope stability and reliability, FLAC simulations were conducted for two different soil conditions: medium-dense and loose. The properties of loose soil are assumed. The properties for the medium-dense soil are detailed in Table 2. For the loose soil, specific assumed soil properties were utilized as follows: friction angle, $\varphi = 30°$, porosity, n = 0.405 and saturated permeability, $k_s = 8.5 \times 10^{-6}$ m/s.

Table 1. Physical properties of silty sand

Soil classification	Specific gravity	Porosity	Dry unit weight (kN/m^3)	Degree of saturation
Silty sand (SM)	2.66	0.33	17.14	0.65

Table 2. Mechanical and hydraulic properties of silty sand

Type	Parameter	Value
Strength properties	c' (kPa)	0
	φ' (°)	34
Elastic properties	E (MPa)	38
	υ	0.35
Hydraulic properties	k_s (m/s)	8.5×10^{-7}
	θ_s	0.37
	θ_r	0.0
	P_0 (kPa)	33.5
	m	1.675

Effect of Rainfall Patterns on Slope Stability

The rainfall data of the Runny Medu rain gauge station is collected from the *State Ground and Surface Water Resources Data Centre*, Chennai, Tamil Nadu, India. The Runny Medu rain gauge station is the closest to Kurumbadi village and is representative of the rainfall at the location. Figure 3 shows the historical rainfall for the year 2009 and Figure 4 shows the different rainfall patterns from 6th November to 11th November 2009. The rainfall volume remains unchanged for other patterns, but the rainfall pattern only changes (Rahimi et al., 2011). The different antecedent rainfall scenarios were considered for analyzing Kurumbai slope stability, including advanced, delayed, normal and uniform, along with the recorded November-2009 pattern. The Factor of Safety (FOS) for the 25° inclined hillslope was evaluated under these rainfall patterns. Figures 5 and 6 illustrate FOS variation with rainfall duration, indicating a faster decrease in FOS for the advanced pattern due to higher initial-rainfall intensity.

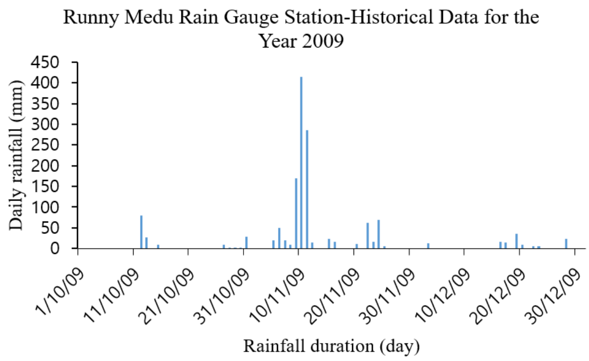

Figure (3): Historical daily rainfall for the year 2009

The delayed and recorded rainfall patterns exhibit an increasing rainfall intensity over time. The gradual increase in rainfall intensity over time results in a corresponding increase in daily-rainfall volume. Initially, this has a minimal effect on matric suction. However, with time, as rainfall volume continues to rise, the pores within the soil become fully saturated with water, causing matric suction to diminish completely. This results in a rapid decline in Factor of Safety (FOS) over time. The FOS values in Figures 5 and 6 stabilize after 96 hours (4 days) of rainfall and consequently, for reliability analysis, only the first 96 hours of rainfall duration are considered.

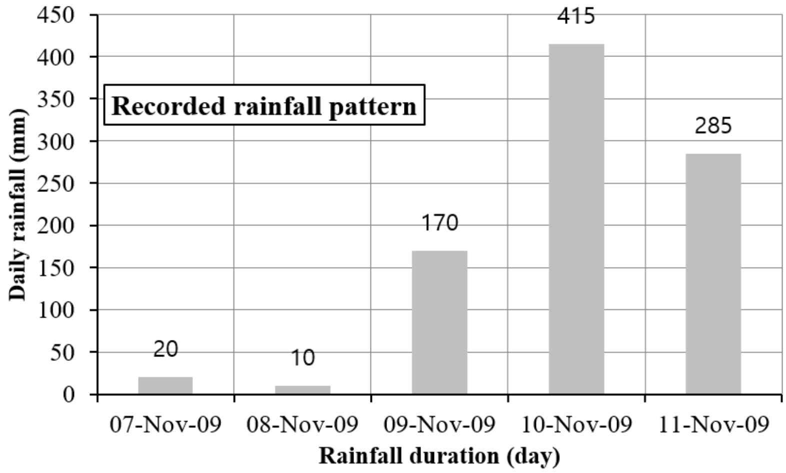
450
400
350
300
250
200
150
100
50
0
Daily rainfall (mm)
Recorded rainfall pattern
415
285
170
20
10
07-Nov-09
08-Nov-09
09-Nov-09
10-Nov-09
11-Nov-09
Rainfall duration (day)

(a)

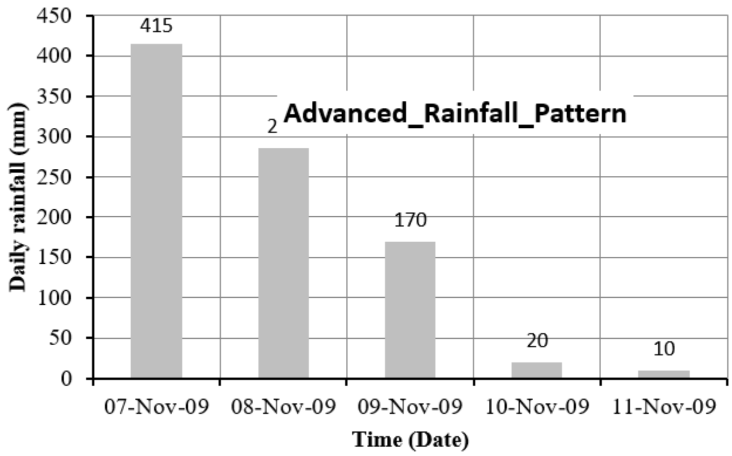
450
400
350
300
250
200
150
100
50
0
Daily rainfall (mm)
415
2
Advanced_Rainfall_Pattern
170
20
10
07-Nov-09
08-Nov-09
09-Nov-09
10-Nov-09
11-Nov-09
Time (Date)

(b)

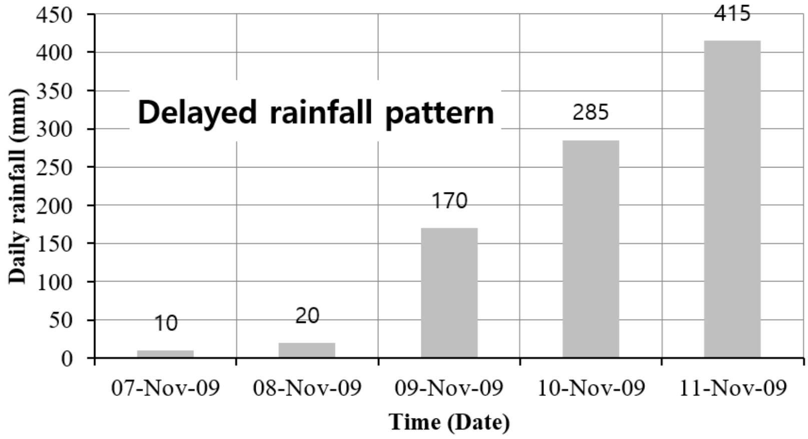
450
400
350
300
250
200
150
100
50
0
Daily rainfall (mm)
Delayed rainfall pattern
415
285
170
10
20
07-Nov-09
08-Nov-09
09-Nov-09
10-Nov-09
11-Nov-09
Time (Date)

(c)

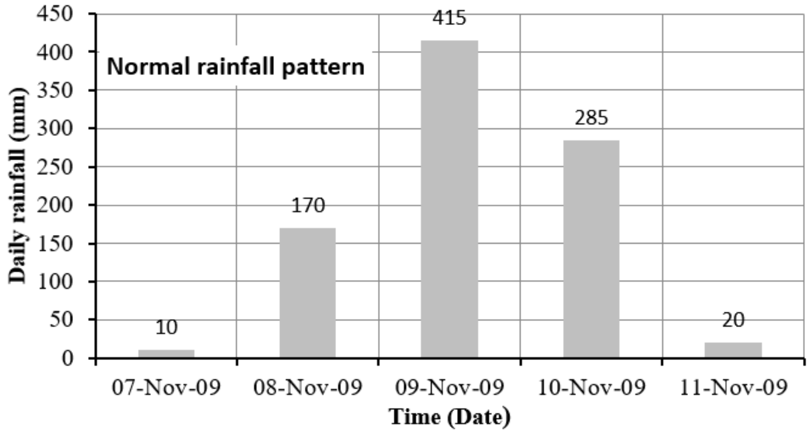

(d)

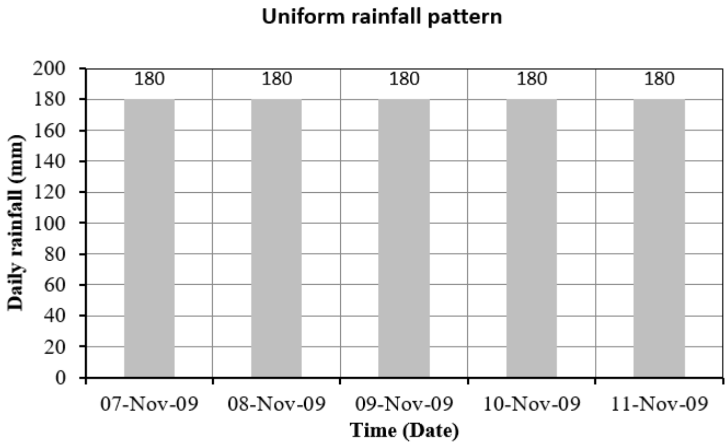

(e)

Figure (4): Rainfall patterns considered in the study: (a) Recorded, (b) Advanced, (c) Delayed, (d) Normal (e) Uniform

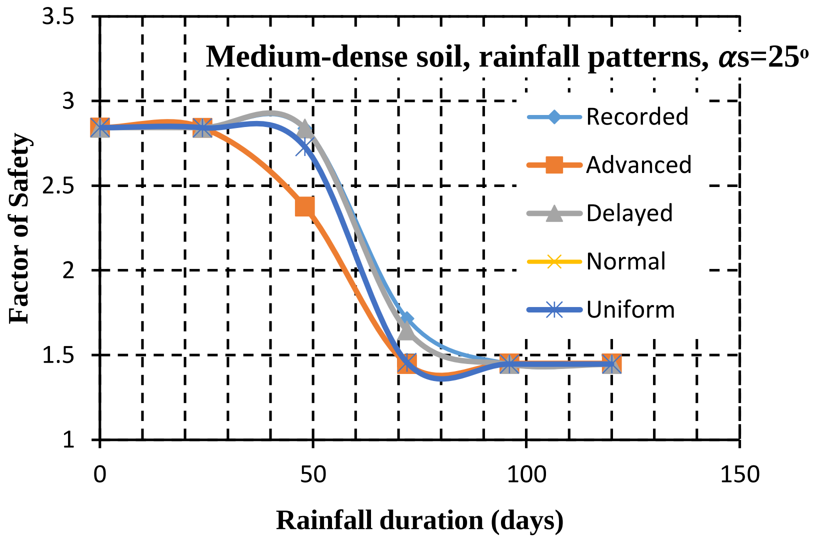

Figure (5): FOS *vs*. rainfall duration for different rainfall patterns for medium-dense soil

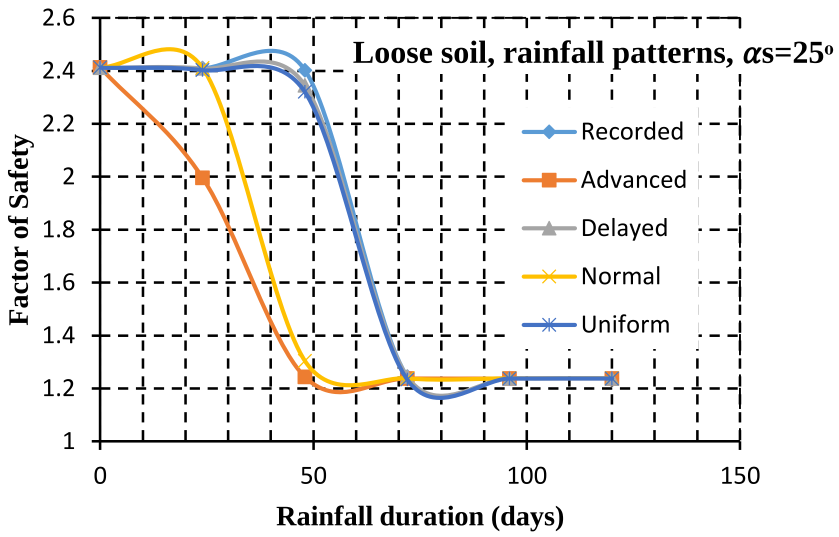

Figure (6): FOS *vs.* rainfall duration for different rainfall patterns for loose soil

Reliability and Probability of Failure

Reliability analysis relies on a performance function (Z), defined as the difference between resistance (R) and load (Q), both functions of random variables. The geotechnical system's performance state involves parameters like X1, X2, …, Xn, representing load and resistance variables and the limit-state function, e.g. for a slope, denoted as g(X1, X2, …, Xn). It can be defined for a particular failure mode as:

$$Z = g(R, Q) = R - Q. \tag{10}$$

The probability of failure is calculated by integrating the joint Probability Density Function (PDF) over all the values of R and Q for correlated random variables. The probability of failure is the probability that the system cannot perform its intended function and is presented mathematically as:

$$P_f = \iint_{g(R,Q)} f_{RQ}\ (r,q)\ dq\ dr \tag{11}$$

where $f_{RQ}\ (r,q)$ is the joint PDF of R and Q.

The integral in Equation (11) is difficult to evaluate and hence can be approximated analytically using the First-order Reliability Method (FORM). The FORM works by transforming the original random variables into standard normal variables with zero mean and unit standard deviation. For the basic variables R and Q, the standard forms are expressed as:

$$Z_R = \frac{R-\mu_R}{\sigma_R} \tag{12}$$

$$Z_Q = \frac{Q-\mu_Q}{\sigma_Q} \tag{13}$$

where μ_R and μ_Q are the mean values of resistance and load, respectively, while σ_R and σ_Q are the standard deviations of resistance and load, respectively.

Definition of Reliability Index

Hasofer and Lind (1974) defined the reliability index as the shortest distance from the origin of reduced variables to the line $g(Z_R, Z_Q) = 0$. The point on $g(Z_R, Z_Q) = 0$ which is closest to the origin is called the design point, as depicted in Fig. 7.The probability of failure can be expressed in terms of the reliability index as:

$$P_f = \Phi(-\beta) \tag{14}$$

where $\Phi(\cdot)$ is the Cumulative Distribution Function (CDF) of the standard normal distribution and β is the reliability index.

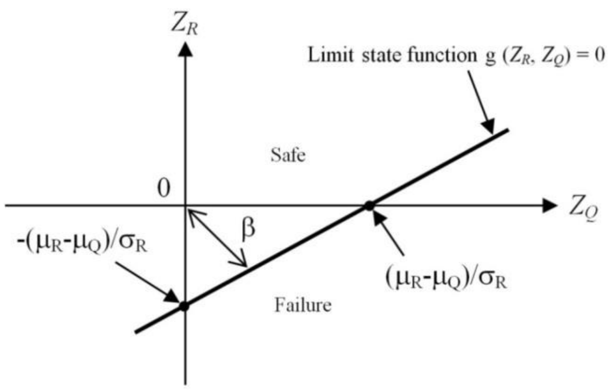

Figure (7): Reliability index as the shortest distance in the space of reduced variables

In the Hasofer and Lind approach, the limit-state function is evaluated at the design point. The design point is not known in advance and therefore, an iteration technique is used to evaluate the design point and thereby calculate the reliability index. The detailed procedure can be found in Nowak and Collins (2013).

Response Surface Methodology

From the foregoing description of the Hasofer and Lind (1974) approach, it is clear that an explicitly stated limit-state function of the system is a prerequisite for the assessment of the reliability index. The RSM is used to approximate the relationship between the input parameters and the response of a system when an explicit relation between the two is not available. Polynomial approximations through Multiple Linear Regression (MLR) usually serve the purpose in the case of geotechnical systems (Babu et al.., 2010; Li et al., 2011; Li et al., 2015). The general approximated relationship can be expressed as:

$$y = f\,(x_1,\, x_2, x_3 \dots) \,+\, e \qquad (15)$$

where e is the least square error, x_i (i= 1, . . ., k) are the k random variables. A limited number of evaluations of the limit-state function (i.e., number of finite-difference runs and infinite slope analyses) are required to build the response surface. In this study, the 2^k factorial design is selected to generate the data required to build the response surface using MLR. In the present study, k = 3 random variables are selected. Design matrix for calculation of FOS is given in Table 3. In Table 3, '+' and '-' correspond to μ+1.65σ and μ-1.65σ, where μ and σ are the mean and standard deviation of the corresponding parameter. These upper bound and lower bound for the different parameters are based upon the assumption that the upper and lower limit values have probabilities of being exceeded by 5% and 95%, respectively. The FOS for each of the combinations in Table 3 is calculated. This set of input and response values is used as training data in MLR to develop the response surface. Based on the values obtained from coefficients of multiple determination (R^2) and adjusted coefficients of multiple determination (R^2_{adj}), the acceptability of the fitted model is checked.

Table 3. Design matrix for calculation of FOS corresponding to 2^k=8 design points in RSM analysis using FLAC

	Friction angle, φ'	Matric suction, ω	Saturate permeability, k_s
1	+	+	+
2	+	+	-
3	+	-	+
4	+	-	-
5	-	+	+
6	-	+	-
7	-	-	+
8	-	-	-

RESULTS AND DISCUSSION

In the reliability analysis for rain-induced slope instability, the commonly used method is the FORM (Tan et al., 2013; Martinovic et al., 2017; Liao and Ji, 2021). This study employs the Response Surface Methodology (RSM) to derive the explicit performance function for reliability analysis, focusing on the Kurumbadi slope. The selected area witnessed a rain-induced landslide on November 10, 2009, causing substantial loss of life and property damage along the Coonoor-Mettupalayam highway in the Nilgiris district. In the analysis, three parameters; namely, friction angle, saturated permeability and matric suction of the soil, are treated as random variables. The Response Surface Methodology is employed to construct the performance function:

$$g(X) = FOS - 1.0. \qquad (16)$$

The regression analysis is carried out for different rainfall durations, *viz.*, t = 0 h, 24 h, 48 h, 72 h and 96 h. For each of the time durations, a linear-regression model is evaluated.

Figure 8 shows the relationship between the probability of failure and rainfall duration for the advanced pattern on the Kurumbadi slope with medium-dense soil at three inclinations. Initial low failure probabilities within the first 3 days suggest adequate matric suction for stability. Beyond 3 days, the 30° slope exhibits higher failure probability, intensifying with increased slope angles. Under advanced rainfall, the maximum failure probability reaches 15.5% for the case of α_s = 30° at 96 h. Figure 9 depicts the fluctuation of failure probability with duration for recorded rainfall, reaching a final 10.3% for the 30° slope, lower than the advanced pattern (P_f = 15.5%). The decreased probability of failure in the recorded rainfall pattern is attributed to lower rainfall intensity (20 mm/day; Fig. 3(a)) towards its end. The differences in failure probabilities between advanced and recorded patterns are minimal, ranging only from 5% to 10%, due to the longer development time of the wetting front in the recorded pattern. Probabilities for all inclinations are less than 2% for rainfall up to 2 days. Beyond 72 h, the 30° slope's failure probability increases drastically. Hence, it can be concluded that the increase in probability of failure with rainfall duration of steeper slopes tends to be much more drastic compared to gentle slopes.

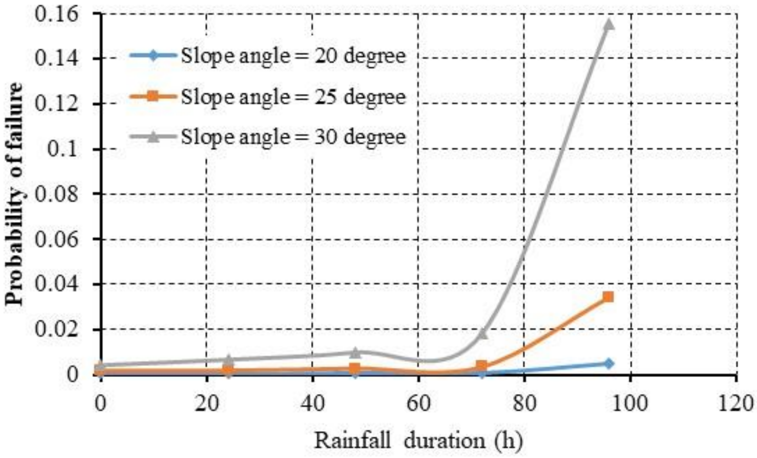

Figure (8): Probability of failure *vs*. rainfall duration of advanced rainfall pattern for the Kurumbadi slope with medium-dense soil

Figures 10 and 11 illustrate failure probabilities for loose soils under advanced and recorded rainfall patterns, respectively. It is observed that there are consistent disparities in failure probabilities between advanced and recorded rainfall patterns, falling within the range from 5% to 10% across various slope angles. This finding suggests that regardless of the specific slope angle, the difference in failure probabilities due to different rainfall patterns remains relatively consistent.

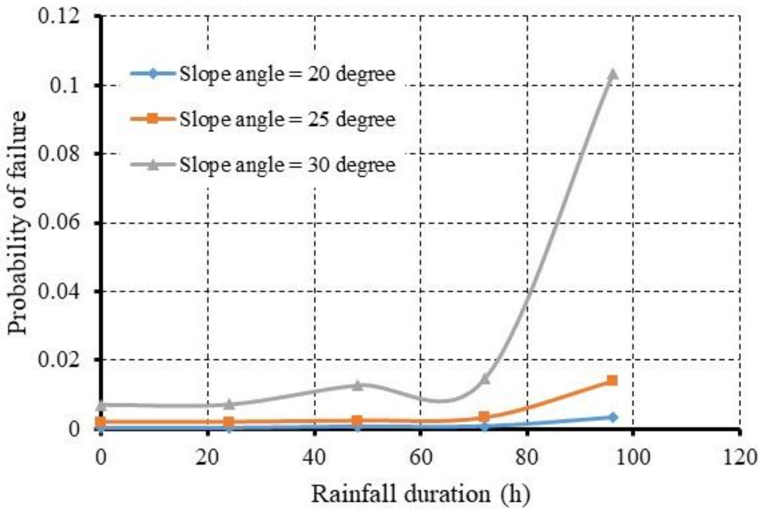

Figure (9): Probability of failure *vs*. rainfall duration of recorded rainfall pattern for the Kurumbadi slope with medium-dense soil

This consistency underscores the significant influence of rainfall patterns and durations on hillslope stability, particularly in loose soils. Such observations are critical for understanding and managing the risks associated with slope instability in regions prone to heavy rainfall or where loose-soil conditions prevail.

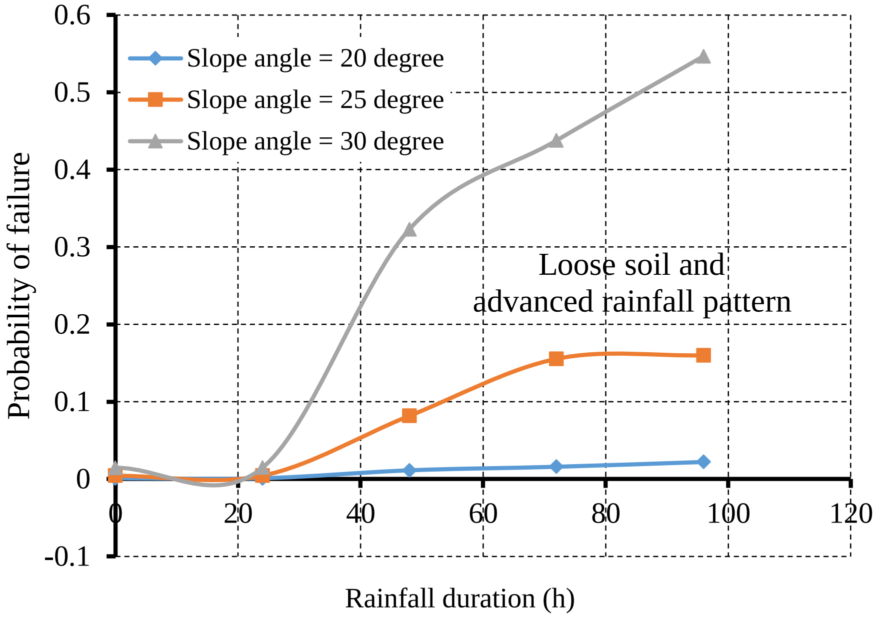

Figure (10): Probability of failure *vs.* rainfall duration of advanced rainfall pattern for the Kurumbadi slope with loose soil

The probability of failure for the hillslope with an inclination of 30° for the advanced rainfall pattern is higher than that corresponding to the recorded rainfall pattern. Probability of failure for loose soil with advanced rainfall pattern is 55%, which is considerably higher than that of medium-dense soil which has the probability of failure of 15.5%. This indicates that the hillslope with loose soil is highly vulnerable for advanced rainfall pattern. Identifying and assessing the slopes along the Coonoor-Mettupalayam highway, which are subject to similar rainfall conditions as the Kurumbadi slope, is crucial due to the potential risks that they pose to both human lives and infrastructure. Given that these slopes share loose soil deposits and similar geometry, there is a heightened risk of instability and slope failure.

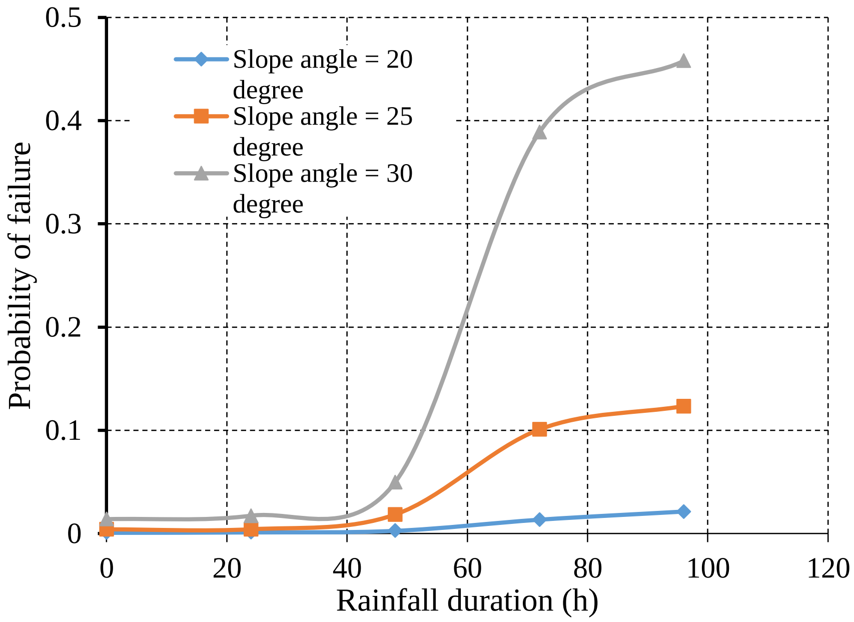

Figure (11): Probability of failure *vs.* rainfall duration of recorded rainfall pattern for the Kurumbadi slope with loose soil

Figure 12 compiles the probability of failure curves of the medium-dense and loose soil slopes in the Kurumbadi region of the Nilgiris district with the slope angle of 30°, subjected to both the advanced and recorded rainfall patterns. These curves serve as valuable early-warning thresholds during rainfall events. By referring to these curves, stakeholders can assess the risk of slope failure and make informed decisions to mitigate potential hazards, offering a proactive approach to managing the impact of rainfall on slope stability in the Kurumbadi region.

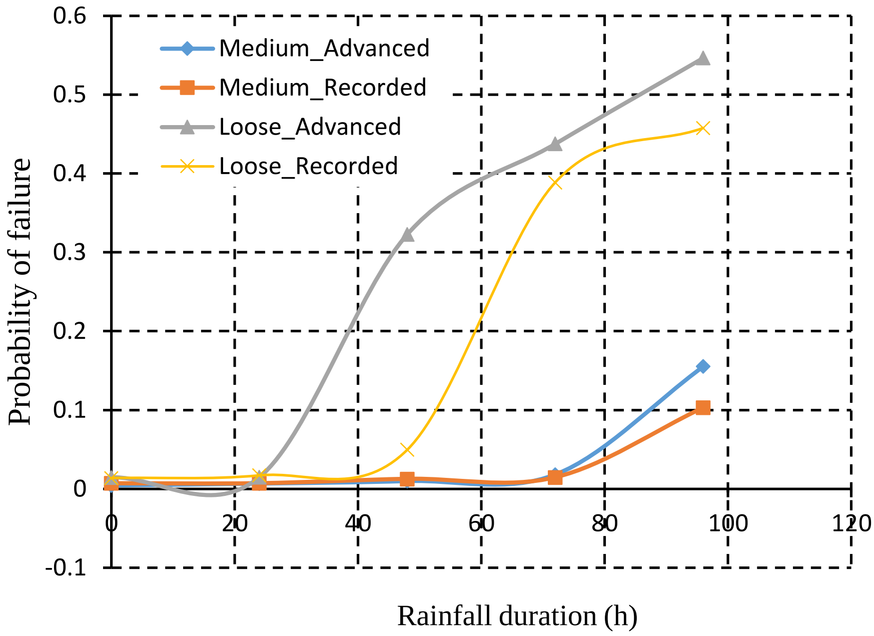

Figure (12): Probability-of-failure curves for the hillslopes of Kurumbadi, the Nilgiris district

CONCLUSIONS

This study focuses on utilizing reliability analysis to assess the impact of rainfall on hillslopes, particularly in the Kurumbadi area of the Nilgiris region. The results, presented in terms of probabilities of failure, concentrate on shallow slope-failure mechanisms using infinite slope analysis. Two distinct rainfall patterns, advanced and recorded, are considered in the analysis, covering slopes with both medium-dense and loose soils. The major conclusions drawn from the study include:

1) An advanced rainfall pattern refers to a scenario where heavy rainfall occurs early in the duration of the event, typically at the onset or within the initial stages of the rainfall event. This pattern is considered one of the worst-possible scenarios for slope stability, because it subjects the soil to intense and sustained moisture infiltration over a shorter period.
2) In the case of both medium-dense and loose soils, this advanced rainfall pattern poses a significant risk. When heavy rainfall occurs early, it saturates the soil quickly, leading to increased pore-water pressure within the soil mass. This elevated pore-water pressure reduces the effective stress within the soil, diminishing its shear strength and stability. As a result, the probability of failure of the slope is relatively higher than those of other rainfall patterns.
3) Additionally, the rapid saturation of the soil due to advanced rainfall pattern leaves less time for natural-drainage processes to occur or for excess water to percolate downward. This further exacerbates the risk of slope failure by maintaining high levels of pore-water pressure within the soil mass.
4) Therefore, the highest probability of failure observed at the end of 96-h rainfall for both medium-dense and loose soils of 15.5 % and 54%, respectively, under advanced rainfall pattern underscores the severity of this scenario and highlights its detrimental impact on slope stability.
5) The decrease in FOS values for medium-dense soil and loose soil for advanced rainfall pattern is from 2.85 to 1.45 and from 2.4 to 1.2, respectively. The

reduction in FOS values indicate a decline in the stability of the slopes, emphasizing the increased susceptibility to failure as a result of the advanced rainfall pattern.

6) The slopes along the Coonoor-Mettupalayam highway, comprised of medium-dense to loose soil deposits and similar geometry as the Kurumbadi slope, pose a serious risk to human lives and infrastructure. Given this heightened risk, it is crucial for relevant authorities and stakeholders to prioritize comprehensive geotechnical assessments and slope-stability analyses along the Coonoor-Mettupalayam highway.
7) The failure-probability curves can be used by engineers along with the detailed weather forecast regarding the likely rainfall intensity and duration, to regulate the vehicle movement and inform the local community about the likelihood of slope failures along the potential landslide prone areas of the Nilgiris district, Tamil Nadu, India.

Conflict of Interests

On behalf of all authors, the corresponding author states that there is no conflict of interests.

REFERENCES

Ali, A., Huang, J., Lyamin, A.V., Sloan, S.W., Griffiths, D.V., Cassidy, M.J., and Li, J.H. (2014). “Simplified quantitative risk assessment of rainfall-induced landslides modelled by infinite slopes.” Engineering Geology, 179, 102-116.

Babu, G.L.S., and Murthy, D.S.N. (2005). “Reliability analysis of unsaturated soil slopes.” Journal of Geotechnical and Geoenvironmental Engineering, 131 (11), 1423-1428.

Babu, G.L.S., and Srivastava, A. (2010). “Reliability analysis of earth dams.” Journal of Geotechnical and Geoenvironmental Engineering, 136 (7), 995-998.

Bouatia, M., Demagh, R., and Derriche, Z. (2023). “Numerical investigation on buried pipelines subjected to permanent ground deformations due to shallow-slope failures.” Jordan Journal of Civil Engineering, 17 (1), 71-82.

Cai. F., and Ugai, K. (2004). “Numerical analysis of rainfall effects on slope stability.” International Journal of Geomechanics, 4 (2), 69-78.

Cai, J.S., Yeh, T.C.J., Yah, E.C., Hao, Y. H., Huang, S.Y. and Wen, J.C. (2017). “Uncertainty of rainfall-induced landslides considering spatial variability of parameters.” Computers and Geotechnics, 87,149-162.

Chatra, A.S., Dodagoudar, G.R., and Maji, V.B. (2017). “Numerical modeling of rainfall effects on the stability of soil slopes.” International Journal of Geotechnical Engineering, 13 (5), 425-437.

Cho, S.E. (2019). “Failure-distribution analysis of shallow landslides under rainfall infiltration based on fragility curves.” Landslides, 10.1007/s10346-019-01257-w

Christian, J.T., Ladd, C.C., and Baecher, G.B. (1994). “Reliability applied to slope-stability analysis.” Journal of Geotechnical and Geoenvironmental Engineering, 120 (12), 2187-2207.

Duncan, J.M. (2000). “Factors of safety and reliability in geotechnical engineering.” Journal of Geotechnical and Geoenvironmental Engineering, 126 (4), 307-316.

Eichenberger, J., Ferrari, A., and Laloui, L. (2013). “Early-warning thresholds for partially saturated slopes in volcanic ashes.” Computers and Geotechnics, 49, 79-89.

FLAC Manual. (2011). “Fluid-mechanical interaction”. Itasca Consulting Group, Inc., Minneapolis.

Hasofer, A.M., and Lind, N.C. (1974) “Exact and invariant second-moment code format.” Journal of Engineering Mechanics, 100, 111-121.

Huang, F., Xiong, H.,Yao, C., Catani, F., Zhou, C., and Huang, J. (2023). “Uncertainties of landslide-susceptibility prediction considering different landslide types.” Journal of Rock Mechanics and Geotechical Engineering. https://doi.org/10.1016/j.jrmge.2023.03.001.

Jaiswal, P., van Westen, C.J., and Jetten, V. (2010). “Quantitative landslide-hazard assessment along a transportation corridor in southern India.” Engineering Geology, 116, 236-250.

Kim, H., Lee, J., Park, H., and Heo J. (2021). "Assessment of temporal probability for rainfall-induced landslides based on nonstationary extreme-value analysis." Engineering Geology, 294. https://doi.org/10.1016/j.enggeo.2021.106372

Li, D.Q., Chen, Y.F., Lu, W.B., and Zhou, C.B. (2011) "Stochastic response-surface method for reliability analysis of rock slopes involving correlated non-normal variables." Computers and Geotechnics, 38 (1), 58-68.

Li, D.Q., Jiang, S.H., Cao, Z.J., Zhou, W., Zhou, C.B., and Zhang, L.M. (2015). "A multiple response-surface method for slope-reliability analysis considering spatial variability of soil properties." Engineering Geology, 187, 60-72.

Liao, W. and Ji, J. (2021). "Time-dependent reliability analysis of rainfall-induced shallow landslides considering spatial variability of soil permeability." Computers and Geotechnics, 129, 1-10.

Martinovic, K., Reale, C., and Gavin, K. (2017). "Fragility curves for rainfall-induced shallow landslides on transport network." Canadian Geotechnical Journal, 55, 852-861.

Mualem, Y. (1976.) "A new model for predicting the hydraulic conductivity of unsaturated porous media." Water Resources Research, 12, 513-522.

Nowak, A.S., and Collins, K.R. (2013). "Reliability of structures". CRC Press, Boca Raton.

Rahimi, A., Rahardjo, H., and Leong, E.C. (2011). "Effect of antecedent rainfall patterns on rainfall-induced slope failure." Journal of Geotechnical and Geoenvironmental Engineering, 137 (5), 483-491.

Raouf, M. A, E., and Bahloul, K.M.M. (2023). "Three-dimensional finite-element analysis of the influence of tunneling on pile foundations." Jordan Journal of Civil Engineering, 17 (4), 598-612.

Shou, K., Wu, C., and Lin, J. (2018). "Predictive analysis of landslide susceptibility under climate-change conditions: A study on the Ai-Liao watershed in southern Taiwan." Journal of Geoengineering, 13, 013-027.

Seshagiri, D.N., and Badrinarayanan, B. (1982) "The Nilgiri landslides: Geological survey of India." Miscellaneous Publications, No. 57.

Tan, X.H., Hu, N., Li, D., Shen, M.F., and Hou, X.L. (2013). "Time-variant reliability analysis of unsaturated-soil slopes under rainfall." Geotechnical and Geological Engineering, 31 (1), 319-327.

Wu, T.H., and Kraft, L.M. (1970). "Safety analysis of slopes". Journal of Soil Mechanics and Foundations Division, 6 (2), 609-630.

Wu, J., and Hsieh, P. (2021). "Numerical assessment of the impact area and the geometry of a landslide dam: The Nan-Shi-Keng landslide, Taiwan." Journal of Geoengineering, 16 (4), 155-167.

Wu, Y., Liu, C., and Lin, B. (2020). "Reliability-based design for deformation-targeted segment of mechanically-stabilized earth wall." Journal of Geoengineering, 15 (1), 1-11.

Wu, M., Wang, J., Chen, J., and Lin, Y. (2021). "A new approach for modeling earthquake magnitude-probability distribution." Journal of Geoengineering, 16 (4), 145-154.